JOURNAL OF THERMOPHYSICS AND HEAT TRANSFER
Vol. 14, No. 2, April–June 2000

Variations of Acoustic and Diffuse Mismatch Models in Predicting Thermal-Boundary Resistance

Lisa De Bellis* and Patrick E. Phelan†
Arizona State University, Tempe, Arizona 85287-6106
and
Ravi S. Prasher‡
Intel Corporation, Chandler, Arizona 85226-3699

Solid-solid thermal-boundary resistance plays an important role in determining heat flow, in both cryogenic and room-temperature applications. The acoustic mismatch model (AMM) and the diffuse mismatch model (DMM) have traditionally been used to predict the thermal boundary resistance R_b across the interface of two adjoining materials at temperatures well below the Debye temperatures of the materials in question. Both the AMM and DMM use the Debye density of states (DOS) in both contacting solids. Here, the use of a measured DOS is made in conjunction with the DMM. This shows an improvement in the prediction of R_b relative to that based on the Debye DOS. Another approach considered is to predict R_b from measured specific heat per unit volume C data. The measured C automatically includes the effect of temperature on the DOS. This leads to a marginal improvement in R_b above that predicted when using the measured DOS. The AMM describes the thermal transport at a solid-solid interface below a few Kelvin quite accurately. The DMM, theoretically more suitable for interfacial transport above a few Kelvin, is no better than AMM for predicting the thermal-boundary resistance at a solid-solid interface. This raises the possibility that both diffuse and specular reflections are taking place at the interface. This kind of mixed reflection is very common in radiative transport. Owing to the similarity in phonon transport and radiative transport a mixed model, considering both specular and diffuse reflection, is developed, which is able to predict R_b values between those of the AMM and DMM. Further, a regime map is developed which delineates three predominant regimes describing the dominance of the R_b predictions made by the AMM, DMM, and mixed models.

Nomenclature

A = area, m^2
a = lattice constant, Å
C = heat capacity per unit volume, $J\ K^{-1}\ m^{-3}$
c = speed of phonons, $m\ s^{-1}$
G = density of states, meV^{-1}
$\hbar$ = Planck's constant divided by $2\pi = 1.055 \times 10^{-34}$ J s
k_b = Boltzmann constant, $1.38062 \times 10^{-23}\ J\ K^{-1}$
N = number of atoms or number of atomic layers
n = atomic density, m^{-3}
$\hat{n}$ = defined in Eq. (19)
Q = heat flow, W
q = heat flux, $W\ m^{-2}$
R_b = thermal-boundary resistance, $m^2\ K\ W^{-1}$
$S_{1\to 2}$ = defined in Eq. (31)
T = temperature, K
α = transmission probability of phonons
Γ = integrated transmission coefficient in the acoustic mismatch model
ΔT = temperature difference, K
δ_d = diffuse reflectivity
δ_s = specular reflectivity
θ = angle of incidence or refraction, rad
θ_d = Debye temperature, K
λ = wavelength, m
ρ = mass density, $kg\ m^{-3}$
ω = phonon angular frequency, $rad\ s^{-1}$
ω_d = Debye frequency, $rad\ s^{-1}$

Subscripts

c = critical
D = properties calculated by Debye model
d = diffuse
i, j = indices
L = longitudinal
s = specular
T = transverse
tot = total
1 = side 1
2 = side 2

Introduction

THERMAL-BOUNDARY resistance R_b results as a consequence of the obstruction of heat flow arising at the interface of two materials, be it liquid-solid interfaces or solid-solid interfaces. At present, the two most widely known models for predicting R_b across a smooth interface at low temperatures are the acoustic mismatch model (AMM) and the diffuse mismatch model (DMM). We find evidence in the literature of the comparison of these models with experimental results.[1,2]

The AMM calculates the transmission coefficient α based on continuum acoustics and the mismatch in the acoustic properties of the materials forming the interface. The DMM calculates α based on the elastic diffuse scattering at the interface. AMM considers specular reflection of phonons at the interface, and DMM considers diffuse reflection at the interface. It is still a matter of debate as to which model is the most representative of a given system. Although for a He/Cu interface DMM and AMM predictions are widely different; for solid-solid interfaces AMM and DMM predictions are very close to each other.[1] Both AMM and DMM are successful in explaining

Received 24 May 1999; revision received 27 October 1999; accepted for publication 29 October 1999.

*Research Assistant, Mechanical and Aerospace Engineering. Student Member AIAA.
†Associate Professor, Mechanical and Aerospace Engineering. Senior Member AIAA.
‡Senior Mechanical Design Engineer, Assembly Technology Development, CH5-157, 5000 W. Chandler Boulevard.

the temperature dependence of R_b at low temperatures, but they have failed at high temperatures. The discrepancies between the models and experimental data can be explained by the simplifying assumptions made in the development of the models and can be improved upon by further enhancement of the models. For example, both models do not consider the scattering near the interface in calculating α.

DMM is theoretically a high-temperature model, as it is based on scattering of phonons at the interface, which is more significant at higher temperatures. Here, the interface appears rough to the phonons because of their short wavelength λ (Ref. 2). Conversely, at low temperatures the interface appears smooth and perfect, and the AMM is better tailored to predict R_b. As it turns out, the DMM and AMM predictions are almost the same for solid-solid interfaces at high temperatures.[1] An exception is the He/Cu interface. The experimental data approach the AMM prediction at extremely low temperatures, and the DMM prediction at relatively high temperatures.[1] Both AMM and DMM predictions are unable to predict data in the intermediate temperatures. Majumdar[3] showed the effect of interfacial roughness on the prediction of R_b for a He/Cu interface. He modified the AMM by considering a fractal model for the surface roughness. These predictions were in excellent agreement with the experimental data. This again makes the issue of the suitability of AMM and DMM more confusing.

Both the AMM and DMM use the Debye density of states (DOS) in both contacting solids. Studies in the literature[2,4] have considered the effect of a more realistic DOS on R_b. In their review paper on R_b, Swartz and Pohl[1] have also recommended the use of a realistic DOS to predict R_b at high temperatures. Phelan[2] incorporated a measured DOS in the DMM to predict R_b between a high-temperature superconductor (HTSC) thin film and its substrate. Phelan's calculation improved the prediction of R_b, edging it closer to experimental data. However, the DOS data were taken at 6 K, and the calculations were performed at temperatures as high as 150 K. Measured DOS of HTSC and other materials are very temperature-dependent,[5] which renders Phelan's calculations a little doubtful. A better approach may be to predict R_b from measured specific heat per unit volume C data. The measured C automatically includes the effect of temperature on the DOS. The foundation of this approach of predicting R_b is based on the work of Swartz and Pohl[1] and Stoner and Maris.[4]

Although AMM and DMM in their original forms are unable to predict R_b for a He/Cu interface, the experimental data fall between the AMM and DMM results.[1] This is also true, in general, for solid-solid interfaces at low temperatures. This raises the possibility that both diffuse and specular reflections are taking place at the interface. This kind of mixed reflection is very common in radiative transport.[6] Owing to the similarity in phonon and radiative transport,[7] a mixed model, considering both specular and diffuse reflection, is developed, which is able to predict R_b values between those of the AMM and DMM.

Predicting R_b

All models presented next stem from the same underlying theory. In all cases our objective is to calculate R_b given by

$$R_b = \Delta T / q_{\text{net}} \tag{1}$$

where ΔT is the temperature difference across the interface $(T_1 - T_2)$ and q_{net} is the net heat transfer per unit area from one side to the other as illustrated in Fig. 1.

From phonon transport theory the total heat Q transferred from one material to another can be expressed as[1,8]

$$Q_{1\to 2} = \frac{1}{2} \cdot \sum_j \int_A \int_{\theta=0}^{\pi/2} \int_{\omega=0}^{\omega_d} N_1(\omega, T_1, j) \cdot \hbar\omega c_{1,j} \alpha_{1\to 2}(\omega) \cos(\theta) \sin(\theta)\, \mathrm{d}\omega\, \mathrm{d}\theta\, \mathrm{d}A \tag{2}$$

The subscripts in $\alpha_{1\to 2}$ denote the transmission probability from material 1 to 2. N_1 is the phonon density that is derived from the Bose–Einstein probability and the Debye DOS[2] and is given by

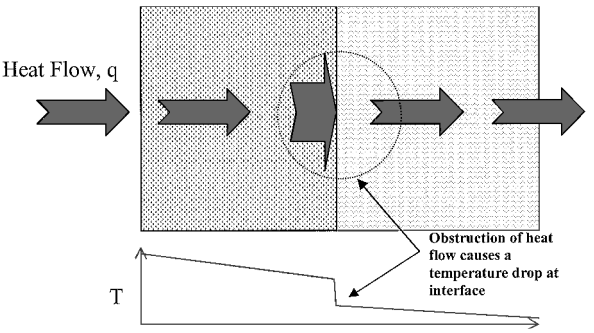

Fig. 1 Thermal-boundary resistance at the interface of two materials in contact.

$$N_1(\omega, T_1, j) = \frac{G_D(\omega, j)}{[\exp(\hbar\omega / k_b T_1) - 1]} \tag{3}$$

where k_b is the Boltzmann constant and G_D is the Debye DOS, given by[9]

$$G_D(\omega, j) = (\omega^2 / 2\pi^2 c_j^3) \tag{4}$$

A similar expression exists for N_2.

To determine the net heat transfer q_{net}, we simply apply the following in conjunction with Eqs. (2–4):

$$q_{\text{net}} = Q_{1\to 2}/A_1 - Q_{2\to 1}/A_2 \tag{5}$$

Slight differences in the evaluation of the integrals in Eq. (2) are considered in each of the models discussed next. In all cases the full details of the derivations will not be repeated but may be found in Refs. 1, 2, and 8.

AMM

The AMM is based on the premise that all of the phonons are specular in nature. Consequently, from AMM theory the transmission coefficient is dependent upon the mode j of the incident phonon, that is, whether it is vibrating longitudinally, parallel transversely, or perpendicular transversely.[10,11] As the transmission coefficient represents the ratio of the transmitted energy to the incident energy, the phenomenon of mode conversion, which occurs at the interface of the two materials, will also affect the value of α. Under the most rigorous calculations three values of α should be considered for each of the three incident modes (although it can be shown that mode conversion does not occur for incident waves vibrating in the perpendicular transverse direction). However, here in the interest of evaluating the feasibility of our proposed model mode conversion is presently not taken into consideration. Further, the assumption is made that the incident waves are traveling at the same speed in all directions. The value of this speed in material 1 is taken as[2]

$$c_1 = \left(\sum_j c_{1,j}^{-2} \right)^{-0.5} = \left(\frac{1}{c_{1,L}^2} + \frac{2}{c_{1,T}^2} \right)^{-0.5} \tag{6}$$

The transmission coefficient in this instance is given by[8]

$$\alpha_{1\to 2} = \frac{4\rho_2 c_2 / \rho_1 c_1 \cdot \cos\theta_2 / \cos\theta_1}{(\rho_2 c_2 / \rho_1 c_1 + \cos\theta_2 / \cos\theta_1)^2} \tag{7}$$

where ρ_i is the density of the ith medium, as indicated, and θ_i is the angle of incidence of the phonon in the ith medium, measured from the normal to the surface. In the rigorous analysis the ratio of the incident to transmitted energies α is found as a consequence of the boundary conditions imposed on the interface; more specifically, the displacement and stress components in the two media must be continuous.[10] The value of α given by Eq. (7) does not, on its own, satisfy these boundary conditions. As stated earlier, this is a consequence of the assumption that no mode conversion occurs at the interface and is recognized as a deficiency.

As the transmission coefficient in the AMM case is dependent upon the angle of incidence, an integrated coefficient Γ is often used. This is given by[8,11]

$$\Gamma_{1\to 2} = \int_0^{\pi/2} \alpha_{1\to 2} \sin\theta \cos\theta \cdot d\theta \tag{8}$$

where $\alpha_{1\to 2}$ is given by Eq. (7). The upper limit of the integral, shown at its maximum possible value of $\pi/2$, is actually dependent upon the two materials under consideration. This critical angle is given by Snell's law:

$$\theta_c = \sin^{-1}(c_1/c_2) \tag{9}$$

Using Eqs. (2–9), the analytical expression for q_{net} is determined as[8,11]

$$q_{\text{net}} = \frac{k_b^4 \pi^2}{60\hbar^3}\left[\frac{\Gamma_{1\to 2}}{c_1^2}(T_1^4 - T_2^4)\right] \tag{10}$$

Equation (10) is slightly modified from that in the cited references in that the average speed defined in Eq. (6) is used in lieu of the longitudinal speed.

The AMM limit for R_b as $\Delta T \to 0$ is given by[1,2]

$$R_b = \left[\frac{k_b^4 \pi^2}{15\hbar^3}\left(\frac{\Gamma_{1\to 2}}{c_1^2}\right)\right]^{-1} T_2^{-3} \tag{11}$$

Again, the value of the longitudinal speed is replaced by the speed defined in Eq. (6).

DMM

The diffuse mismatch theory considers the case where all phonons are diffuse. In this particular instance the transmission coefficient is no longer dependent on the angle of incidence. Based on this, one can derive an expression for the transmission coefficient α. The details will not be repeated here but can be found in Ref. 2. The transmission coefficient is given by[1,2]

$$\alpha_{1\to 2} = \frac{\sum_j c_{2,j}^{-2}}{\sum_j c_{1,j}^{-2} + \sum_j c_{2,j}^{-2}} \tag{12}$$

where c is the speed of sound through medium 1 or 2, as indicated, for the jth transmission mode (polarization). Also of importance is the following relation[1]:

$$\alpha_{1\to 2} + \alpha_{2\to 1} = 1 \tag{13}$$

Substituting Eqs. (2), (3), (4), (12), and (13) into (5) will yield the following analytical expression for q_{net} (Refs. 1 and 2):

$$q_{\text{net}} = \frac{k_b^4 \pi^2}{120\hbar^3}\left(T_1^4 \sum_j c_{1,j}^{-2}\alpha_{1\to 2} - T_2^4 \sum_j c_{2,j}^{-2}\alpha_{2\to 1}\right) \tag{14}$$

In the limit where the temperature difference between the two materials approaches zero, Eq. (14) becomes[1,2]

$$R_b = \left[\frac{k_b^4 \pi^2}{30\hbar^3}\left(\sum_j c_{1,j}^{-2}\right)\alpha_{1\to 2}\right]^{-1} T_2^{-3} \tag{15}$$

Prediction of R_b Using Measured Density of States and Specific Heat

Theoretically the incorporation of a measured DOS, or a more realistic theoretical DOS, is possible by direct substitution of the DOS into Eq. (2), but it results in further complications. With the use of the Debye DOS [Eq. (4)] and excluding near-surface scattering, α is independent of temperature and frequency. Under these assumptions the speed with which the phonons travel is also independent of frequency, but with a realistic DOS the speed of the phonons is basically the group speed of the lattice waves. The group speed is not only frequency dependent but also direction dependent for materials like YBCO.[4] Stoner and Maris[4] considered a detailed model for face-centered cubic (FCC) materials. Their analysis showed the importance of considering a realistic DOS on the prediction of R_b. Stoner and Maris's approach, although theoretically quite straightforward, is mathematically too cumbersome. Furthermore their analysis is also entirely theoretical, and thus the group speed and α can be easily estimated, which is not the case when attempting to incorporate a measured DOS.

The measured DOS generally differs from a detailed theoretical calculation of the DOS.[12] Rhyne et al.[13] have shown that the shape of the measured DOS is quite different for measurements conducted at different temperatures. Furthermore, the measured DOS has a number of peaks and valleys, which, when numerically integrated, lead to some amount of uncertainty. This complicates the matter further, and some simplifying assumptions are typically made to include the effect of the measured DOS. Phelan[2] included the effect of the measured DOS by assuming α to be the same as that given by the DMM and that Eq. (12) holds while using the measured DOS. The main drawback of his calculation is that it implicitly assumes the same form of the DOS on both sides of the material. However, at the temperatures under consideration, the Debye DOS is uniquely appropriate for the substrate side.[4] Using Eqs. (2) and (5) and assuming α to be given by Eq. (12), q can be expressed as[2]

$$q = \frac{\hbar\alpha_{1\to 2}}{4}\sum_j c_{1,j}\int_0^{\omega_c} G(\omega, j)\omega\left[\frac{1}{\exp(\hbar\omega/k_bT_1) - 1} - \frac{1}{\exp(\hbar\omega/k_bT_2) - 1}\right] d\omega \tag{16}$$

where ω_c is the cutoff frequency. The measured DOS includes the contributions from all of the modes. Therefore, if the assumption is made that all of the modes contribute equally to the total DOS (G_{tot}), then

$$G(\omega, j) = G_{\text{tot}}(\omega)/3 \tag{17}$$

Substitution of Eq. (17) into Eq. (16) results in

$$q = \frac{\hbar\alpha_{1\to 2}}{12}\sum_j c_{1,j}\int_0^{\omega_c} G_{\text{tot}}(\omega)\omega\left[\frac{1}{\exp(\hbar\omega/k_bT_1) - 1} - \frac{1}{\exp(\hbar\omega/k_bT_2) - 1}\right] d\omega \tag{18}$$

Phelan[2] used the DOS data for YBCO from Gompf et al.[14] to calculate the R_b across a YBCO/MgO interface. Measured values of G_{tot} are reported in units of meV^{-1}. To establish G_{tot} on a per-unit-volume basis, these values are multiplied by a factor $\hat{n}$, defined by[15]

$$\hat{n} = \frac{\text{number of primitive cells}}{\text{unit volume}} \tag{19}$$

The definition of the number of primitive cells is a bit confusing for a material like YBCO because it has three different lattice constants in the three directions[2] and also has 13 atoms in one unit cell. Phelan[2] assumed the primitive cell to be the same as the unit cell and hence neglected the effect of the 13 atoms in one unit cell. In this analysis an effective lattice constant[16] is used, which represents a unit cell containing only 1 atom, and therefore the number of primitive cells is the same as the number of unit cells. This approach also leads to a theoretical Debye temperature, which is closer to the experimental Debye temperature than that used by Phelan.[2] The equivalent lattice constant a is given by[16]

$$a = \pi/(6\pi^2 n)^{\frac{1}{3}} \tag{20}$$

The data for both YBCO and MgO are taken from Ref. 2 and shown in Table 1. Using Eqs. (19) and (20) results in $a = 1.91$ Å and

Table 1 Physical properties of materials[2,22]

Material	Longitudinal sound speed, c_L, m s^{-1}	Transverse sound speed, c_T, m s^{-1}	Mass density, ρ, kg m^{-3}
YBCO	4780	3010	6338
MgO	9710	6050	3576
Copper	4830	2390	9020
^{3}He solid	580	210	128

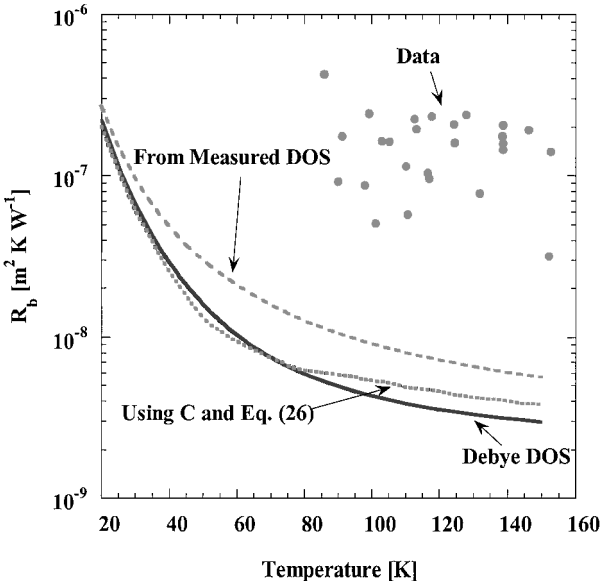

Fig. 2 R_b predictions for a YBCO/MgO interface by the incorporation of the measured DOS, or C, with experimental data.[17]

$\hat{n} = 1.435 \times 10^{29}$ m^{-3}. After proper conversion of G_{tot} to appropriate units, R_b is calculated and is shown in Fig. 2, along with the experimental data[17] and the theoretical DMM calculation using the Debye DOS [Eq. (4)]. It shows an improvement in the prediction of R_b relative to that based on the Debye DOS. Unfortunately, there is a large uncertainty in the calculation because G_{tot} was measured at 6 K, whereas calculations are carried out to temperatures well above that. As already mentioned, G of YBCO is strongly dependent on temperature.[5] Aral et al.[18] have also studied and shown a substantial difference in the magnitude of G for HTSC at different temperatures. The temperature dependence of G can be circumvented by using measured values of the specific heat C instead of G.

In terms of G_{tot}, C is given by[2]

$$C = \frac{\mathrm{d}}{\mathrm{d}T}\left[\int_0^{\omega_c} \frac{G_{\text{tot}}(\omega, j)\hbar\omega}{\exp(\hbar\omega/k_bT) - 1}\right] \tag{21}$$

Substitution of Eq. (21) in Eq. (18) leads to

$$q = \frac{\alpha_{1\to 2}}{12}\sum_j c_{1,j}\int_{T_2}^{T_1} C_1\,\mathrm{d}T \tag{22}$$

Because $\Delta T \to 0$, C_1 can be removed from the integral, and Eq. (22) simplifies to

$$\frac{q}{\Delta T} = \frac{\alpha_{1\to 2}}{12}\sum_j c_{1,j}C_1(T) \tag{23}$$

giving us

$$R_b = \left(\frac{\alpha_{1\to 2}}{12}\sum_j c_{1,j}\right)^{-1} C_1(T)^{-1} \tag{24}$$

Instead of using the measured DOS, R_b can be predicted from the measured values of C. The data for C that we use for YBCO are those of Roulin et al.[19] The R_b relation in Eq. (24), at low temperatures, should reduce to that of the DMM using the Debye DOS given by Eq. (15) (Ref. 20). However, in doing so we find that it does not reduce to an equivalent relation. The reason for this is that all of the polarizations are assumed to contribute equally to G_{tot}, but if the speeds of different polarizations are different, then their contributions to G_{tot} will not be the same. We may, therefore, compute G along different polarizations as follows:

$$G(\omega, j) = \tfrac{1}{3}(c_D^3/c_j^3)G_{\text{tot}}(\omega) \tag{25}$$

If the speeds of phonons along all of the polarizations are the same, then Eq. (25) reduces to Eq. (17). Substituting Eq. (25) into Eq. (18) and using the definition of C from Eq. (21) yields

$$R_b = \left(\frac{\alpha_{1\to 2_d}}{12}c_{1_D}^3\sum_j c_{1,j}^{-2}\right)^{-1} C_1(T)^{-1} \tag{26}$$

If the formula for the Debye specific heat is substituted into Eq. (26), it reduces to the appropriate form. Calculations using Eq. (26) are also shown in Fig. 2. Use of Eq. (26) leads to a marginal improvement in R_b above that predicted when using G as defined in Eq. (17). Equation (25) will lead to a vastly different result than Eq. (17) if the speeds of the phonons along different polarizations are largely different, but this is not the case with YBCO.

Figure 2 shows that the predictions of R_b from all of the different models considered here match very well at low temperatures, which is expected. The use of the effective lattice constant is appropriate for YBCO. In Phelan's[2] calculation the prediction of R_b from the measured DOS does not match the Debye DOS predictions, even at very low temperatures. Here, at higher temperatures, the predicted values of R_b from the specific heat and measured DOS do not match. Some of the apparent reasons are the following:

1) The specific heat and the DOS data are not for the same samples. These data are also from different research groups.

2) DOS was measured at 6 K, and therefore the R_b prediction by using measured C and G are in agreement only at low temperatures. This really makes the use of the measured DOS a little suspect. However, the prediction of R_b from the measured C is not any better than that using the Debye DOS. This is also because the measured C is approximately the same as that predicted by considering the Debye DOS.

Until now the analysis using the measured DOS implicitly assumed the same form of DOS on both sides of the interface. However, for most substrate materials the Debye DOS is still valid owing to their very high Debye temperature θ_d (Refs. 4 and 21). One advantage of assuming the same DOS on both sides and using α given by Eq. (12) is that it satisfies the law of detailed balance. The law of detailed balance basically means that the number of phonons of frequency ω crossing the interface from side 1 to side 2 is the same as the number of phonons crossing from side 2 to side 1 (Ref. 1). The law of detailed balance holds only for elastic scattering.[21] If the law of detailed balance is relaxed and the true representative DOS of material 2 or of the substrate is assumed, then an alternative form of α can be derived. Starting with the basic definition of $q_{1\to 2}$ and $q_{2\to 1}$, assuming α to be independent of ω and θ, one can easily see that

$$a_{1\to 2} = \sum_j \int_0^{\omega_c} \frac{G_2(\omega, j)\omega c_{2,j}}{\exp(\hbar\omega/k_bT) - 1}\,\mathrm{d}\omega$$

$$\Bigg/ \left[\sum_j \int_0^{\omega_c} \frac{G_1(\omega, j)\omega c_{1,j}}{\exp(\hbar\omega/k_bT) - 1}\,\mathrm{d}\omega\right.$$

$$\left. + \sum_j \int_0^{\omega_c} \frac{G_2(\omega, j)\omega c_{2,j}}{\exp(\hbar\omega/k_bT) - 1}\,\mathrm{d}\omega\right] \tag{27}$$

The preceding relation results in a temperature-dependent α.

As discussed earlier, the substrate remains in the Debye regime for a long range of temperatures, and thus G_2 is basically the Debye

DOS. Because the substrate is still in the Debye regime, ω_c in the expression for the substrate in Eq. (27) can be conveniently replaced by its ω_d. The reason for this is that ω_c or ω_d is effectively infinity in the Debye regime.[21] From the definition of C in Eq. (21), Eq. (27) can be reduced to

$$\alpha_{1\to 2} = \frac{\Sigma_j c_{2,j} \int_0^T C_{2_D}(T)\,\mathrm{d}T}{C_{1_D}^3 \Sigma_j c_{1,j}^{-2} \int_0^T C_1(T)\,\mathrm{d}T + \Sigma_j c_{2,j} \int_0^T C_{2_D}(T)\,\mathrm{d}T} \tag{28}$$

where C_{2_D} is the Debye specific heat of material 2. Calculation of R_b using this expression for α, however, does not lead to any improvement over that predicted by Eq. (26). The reason for this is that the predictions of R_b from Eq. (26) and that using the Debye DOS on both sides are almost the same for YBCO/MgO interfaces. C for YBCO is approximately the same as that predicted by the Debye DOS. Therefore Eq. (28) effectively reduces to Eq. (11), i.e., the original DMM case. If the assumptions of constant C and the same c for all polarizations are made, then Eq. (28) reduces to

$$\alpha_{1\to 2} = \frac{c_2 C_{2_D}(T)}{c_1 C_1(T) + c_2 C_{2_D}(T)} \tag{29}$$

which is exactly the same as that suggested by Chen[21] for inelastic scattering at the interface. Because this model does not lead to any improvement in the prediction of R_b, it is not shown in Fig. 2.

Prediction of R_b Using a Mixed Model

As stated earlier, the DMM assumes that the phonons are diffusely transmitted, whereas the AMM assumes specular transmission. The fraction of diffuse or specular transmission is dependent on the materials under investigation. The applicability of either the AMM or DMM can be determined by the ratio of the dominant phonon wavelength to the mean interfacial roughness of the two media.[2] As demonstrated by Chen,[16] in the interest of considering the most general of cases, a means for addressing the possibility of either specular or diffuse transmission should be adopted. Chen[16] applies this approach to superlattices, whereby an assumed interface scattering parameter p is used to represent the fraction of specularly reflected phonons at the interface. The model described here differs in that specular or diffuse transmission is based upon the material properties. This mixed model allows us to incorporate both forms of transmission.

Physically, the transmission of phonons is not likely to be purely specular or diffuse, but rather a combination of the two. Figure 3 illustrates the physical difference between these two modes of transmitted energy. We see in Fig. 3 the critical cone resulting from the angle dependence of the transmission coefficient in the specular case. A criterion for judging whether the phonon should be diffusely or specularly transmitted must be defined. To do this, we turn to the analogous case in radiation heat transfer. We find in the literature an expression for the probability S of specular reflection of a photon[6]:

$$S = \delta_s/(\delta_s + \delta_d) \tag{30}$$

Equation (30) simply represents the relative probability that a specular reflection occurs given the possibility of either a diffuse or specular reflection. The analogy between photons and phonons is valid and has been employed in the literature.[7,15] Thus, Eq. (30) is used here. Given a real surface, it would be extremely difficult to judge the degree of specular and/or diffuse behavior. As an alternative to making an educated guess and setting the values to a predetermined percentage of diffuse to specular transmission, Eq. (30) provides a measure that would introduce some degree of randomness and which in some way reflects the materials being used. In the absence of absorption, the sum of the transmissivity and the reflectivity must be unity. Thus, in our model we can employ an analogous ratio given the transmission coefficients for both the AMM and DMM. Initially, the ratios of reflectivities as in the case of radiation heat transfer were implemented. However, this procedure was found to violate the second law of thermodynamics. When applying the same procedure with the ratios of transmissivities, the second law was, in fact, satisfied. In the interest of consistency, Eq. (8) is also employed to calculate an integrated transmission coefficient for the DMM or diffuse case ($\Gamma_{d,1\to 2}$). Here, $\alpha_{1\to 2}$ is given by Eq. (12), and as it is independent of the angle of incidence, it can be removed from the integral in Eq. (8).

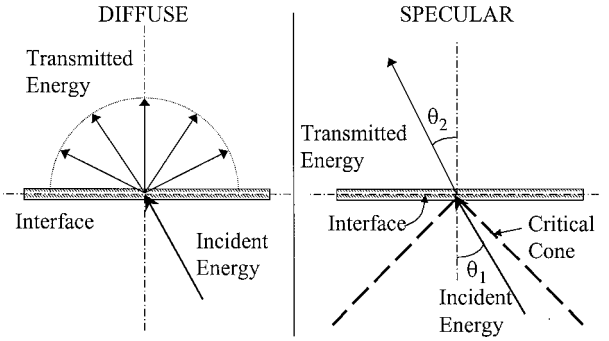

Fig. 3 Diffuse vs specular transmission at an interface.

Therefore the probability $S_{1\to 2}$ that a phonon is specular is given by

$$S_{1\to 2} = \frac{\Gamma_{s,1\to 2}}{\Gamma_{s,1\to 2} + \Gamma_{d,1\to 2}} \tag{31}$$

Reviewing the derivations of all of the models just discussed, attention was focused upon the expression for the phonon number density N_1, given by Eq. (3). According to Ashcroft and Mermin,[15] this represents the total number of phonons present in thermal equilibrium at temperature T. From here, we can then assume that among these phonons some of these are specular $N_{s,1}$ and some are diffuse $N_{d,1}$.

Using Eq. (31), we can express the ratio of specular to total phonons and in this way derive the following expression for N_1:

$$N_1 = N_{s,1} + N_{d,1} = \left(\frac{\Gamma_{s,1\to 2}}{\Gamma_{s,1\to 2} + \Gamma_{d,1\to 2}}\right) \cdot N_1 + \left(\frac{\Gamma_{d,1\to 2}}{\Gamma_{s,1\to 2} + \Gamma_{d,1\to 2}}\right) \cdot N_1 \tag{32}$$

A similar expression can be written for N_2. If we substitute Eq. (32) into Eq. (2), and subsequently Eq. (5), we obtain the following expression for q_{net}:

$$q_{\text{net}} = \frac{k_b^4 \pi^2}{60\hbar^3}\left[\sum_j c_{1,j}^{-2}\left(\frac{\Gamma_{s,1\to 2}^2 + \Gamma_{d,1\to 2}^2}{\Gamma_{s,1\to 2} + \Gamma_{d,1\to 2}}\right)\right](T_1^4 - T_2^4) \tag{33}$$

The approach taken to obtain Eq. (33) was verified to satisfy the second law of thermodynamics. By substituting Eq. (33) into the definition of R_b, Eq. (1), and making the usual low temperature approximation,[1] i.e., T_2 is very small compared to the Debye temperature, the expression for R_b simplifies to

$$R_b = \left\{\frac{\pi^2}{15}\frac{k_b^4}{\hbar^3}\left[c_{1,j}^{-2} \cdot \left(\frac{\Gamma_{d,1\to 2}^2 + \Gamma_{s,1\to 2}^2}{\Gamma_{d,1\to 2} + \Gamma_{s,1\to 2}}\right)\right]\right\}^{-1} T_2^{-3} \tag{34}$$

Calculations using the mixed model are performed for a solid ^{3}He/Cu interface and are shown in Fig. 4. Physical data for the solid ^{3}He and Cu were taken from Folinsbee and Anderson[22] and are listed in Table 1. Here, the calculations given by the DMM and AMM cases, as well as the mixed model case, are plotted along with the experimental data from Anderson et al.[23] Figure 4 shows that both AMM and DMM predictions are vastly different and the experimental data lie between the AMM and DMM results. The

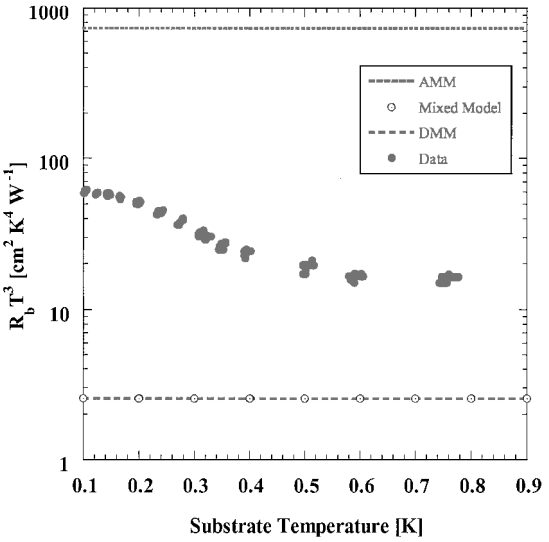

Fig. 4 Comparison of R_b predictions for a He-3 solid/Cu interface by the AMM, DMM, and mixed model with experimental data.[23]

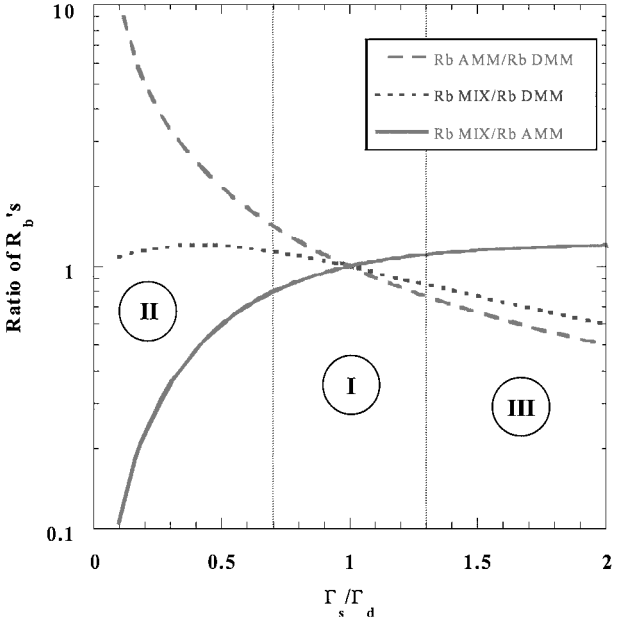

Fig. 5 Regime map depicting areas best suited for AMM, DMM, and mixed model analyses.

experimental data are slightly closer to the AMM predictions at very low temperatures but edge closer to the DMM predictions with increasing temperature. Though not readily evident in Fig. 4, the mixed model results lie within the AMM and DMM curves. The mixed model prediction is very close to the DMM prediction (2.5471 vs 2.5384, respectively) for ^{3}He/Cu because the critical angle of ^{3}He is extremely small. Therefore phonons are primarily transported across the interface diffusely from outside the critical cone.

The mixed model also lacks in predicting the correct temperature dependence of R_b because its foundation is essentially the same as that of the AMM and DMM. Majumdar[3] showed that the apparent roughness for the phonons striking the interface is frequency dependent, which effectively results in an increase in the area of the interface as the temperature increases. The enhanced transmission of phonons because of Rayleigh scattering[3] also reduces R_b, resulting in an R_b lower than that predicted by AMM.

Overall the agreement between these data and the predictions made by all of the models considered is not very good. Swartz and Pohl[1] suspect that this trend is a consequence of inelastic phonon scattering resulting from local asperities on the material surfaces. They explain that this trend is not intrinsic to R_b and is, therefore, difficult to account for in the models. This is supported by experiments conducted by Olson and Pohl.[24] They measured the phonon transmission across the interface and the scattering rate at the solid interface simultaneously for a Silicon/^{4}He interface, which was either polished, ion-etched, or coated with SiO_2. They were able to demonstrate good agreement with the AMM for the polished sample at temperatures below 0.3 K. Above that temperature, discrepancies existed that were supported by the residual diffuse phonon scattering observed during the experimentation. The R_b of the etched sample, expected to contribute to diffuse scattering because of its surface treatment, did in fact edge closer to the DMM limit. This work demonstrated that a range of R_b is observable within the predicted limits when different surface treatments and phonon wavelengths are used. It also demonstrates the difficulty in physically measuring a real surface, especially a thin film/substrate interface, to determine how specular/diffuse it may be. For this reason the mixed model is not based on actual physical measurements of the surface roughness. Rather, the physical basis for this approach is that the second law is always satisfied.

Also, the models discussed here calculate R_b based on the temperature of the incident phonons. However, Chen[25] makes the distinction between this temperature and that of the equilibrium temperature of the surface. The two are not equivalent, and the value of R_b will be effected by the temperature considered. Typically, in experimental work, the equilibrium temperature is recorded.

The neglect of scattering near the interface presents a possible means of improvement. This is confirmed by Swartz and Pohl,[1] who suggest that the effects of inelastic scattering should be investigated for higher temperatures.

Regime Map

As demonstrated by the results in Fig. 4, the mixed model prediction for R_b is almost indistinguishable from that of the DMM prediction for the He/Cu interface, while both these models are orders of magnitude lower than the AMM prediction. This raises the question of the applicability of each model. To answer this, a regime map is developed and depicted in Fig. 5. Swartz and Pohl[1] also presented a regime map of sorts in their review of thermal-boundary resistance that plots the ratio of R_b vs the dissimilarity. Their plot, however, is only of a qualitative nature, where the dissimilarity, which refers to the amount of mismatch, is plotted along the abscissa using an arbitrary scale. The regime map presented here plots ratios of R_b as predicted by all of the models just discussed in different combinations vs the ratio of the integrated transmission coefficient for the specular (or AMM) case over that of the diffuse (or DMM) case. Unlike the plot presented by Swartz and Pohl,[1] the abscissa involves a quantitative scale, the value of which can be easily calculated for any two materials under consideration. Plotting the ratio of R_bs removes the temperature dependence of the data. From Fig. 5 we can recognize three regimes. The first occurs when the ratio Γ_s/Γ_d is unity. At this point all curves converge, demonstrating that all models predict the same value of R_b. The second regime occurs for $\Gamma_s/\Gamma_d < 1$. In this regime the AMM prediction for R_b is clearly greatest, while the ratio of the MIX to DMM model predictions is close to unity. This supports the results obtained for the ^{3}He/Cu interface just discussed. For small values of Γ_s relative to Γ_d, the AMM prediction is very large compared to the other models, whose predictions are essentially equivalent. The last regime, occurring when $\Gamma_s/\Gamma_d > 1$, reveals that the DMM prediction is larger than that of the other models, although the difference is nowhere near as dramatic as in the case of the AMM dominance in regime II. We may also conclude from Fig. 5 that the R_b prediction made by the MIX model is closest to that of the DMM case when $\Gamma_s/\Gamma_d < 1$ and closest to the AMM prediction when $\Gamma_s/\Gamma_d > 1$. Although not shown on Fig. 5, all curves asymptote horizontally beyond $\Gamma_s/\Gamma_d = 2$. As Γ_s and Γ_d depend on the materials under consideration, one can easily determine, with the use of Fig. 5, the caliber of the predictions each model will make without actually calculating R_b.

Conclusions

This paper explores the various possibilities of predicting R_b from measured DOS and measured C. However, the inclusion of the measured DOS and the prediction from the measured C for YBCO/MgO still do not yield values of R_b anywhere close to the experimental data. An analytical mixed model is also developed, which considers both the specular and diffuse reflection of phonons at the interface. The predictions of the mixed model are between those of the original AMM and DMM predictions, although these still are not representative of the experimental data. This further substantiates the importance of near-surface scattering on the prediction of R_b. Considering the calculations in this paper and the calculation by others in the past,[4] it seems scattering is a far more dominant determinant in predicting R_b.

A regime map is charted that outlines the nature of the R_b predictions made by the models discussed here. This map depends solely on the material properties of the interface and is independent of temperature.

Acknowledgments

P. E. Phelan gratefully acknowledges the support of the National Science Foundation through an NSF CAREER Award (Grant CTS-9696003) and the financial support of the Raytheon Corporation.

References

[1]Swartz, E. T., and Pohl, R. O., "Thermal Boundary Resistance," *Reviews of Modern Physics*, Vol. 61, No. 3, 1989, pp. 605–668.

[2]Phelan, P. E., "Application of Diffuse Mismatch Theory to the Prediction of Thermal Boundary Resistance in Thin-Film High—T_c Superconductors," *Journal of Heat Transfer*, Vol. 120, No. 1, 1998, pp. 37–43.

[3]Majumdar, A., "Effect of Interfacial Roughness on Phonon Radiative Heat Conduction," *Journal of Heat Transfer*, Vol. 113, No. 4, 1991, pp. 797–805.

[4]Stoner, R. J., and Maris, H. J., "Kapitza Conductance and Heat Flow Between Solids at Temperature from 50 to 300 K," *Physical Review B*, Vol. 48, No. 22, 1993, pp. 16,373–16,387.

[5]Mase, S., "Phonons in High T_c Superconductors," *Studies of High Temperature Superconductors*, Nova Science Publishers, New York, 1989, pp. 129–168.

[6]Palmer, B. J., Drost, M. K., and Welt, J. R., "Monte Carlo Simulation of Radiative Heat Transfer in Arrays of Fixed Discrete Surfaces Using Cell-to-Cell Photon Transport," *International Journal of Heat and Mass Transfer*, Vol. 39, No. 13, 1996, pp. 2811–2819.

[7]Majumdar, A., "Microscale Heat Conduction in Dielectric Thin Films," *Journal of Heat Transfer*, Vol. 115, No. 1, 1993, pp. 7–16.

[8]Little, W. A., "The Transport of Heat Between Dissimilar Solids at Low Temperatures," *Canadian Journal of Physics*, Vol. 37, 1959, pp. 334–349.

[9]Kittel, C., *Introduction to Solid State Physics*, Wiley (SEA), PTE LTD, Singapore, 1986, pp. 80–124.

[10]Cheeke, J. D. N., Hebral, B., and Martinon, C., "Transfert de Chaleur Entre Deux Solides en Dessous de 100 K," *Le Journal de Physique*, Vol. 34, 1973, pp. 257–272.

[11]Cheeke, J. D. N., Ettinger, H., and Hebral, B., "Analysis of Heat Transfer Between Solids at Low Temperatures," *Canadian Journal of Physics*, Vol. 54, 1976, pp. 1749–1771.

[12]Ziman, J. M., *Electrons and Phonons*, Oxford Univ. Press, London, 1960, pp. 288–333.

[13]Rhyne, J. J., Neumann, D. A., Gotaas, J. A., Beech, F., Toth, L., Lawrence, S., Wolf, S., Osofsky, M., and Gubser, D. U., "Phonon Density States of Superconducting Yba2Cu3O7 and the NonSuperconducting Analog Yba2Cu3O6," *Physical Review B*, Vol. 36, No. 4, 1987, pp. 2294–2297.

[14]Gompf, F., Renker, B., and Gering, E., "Comparison of the Phonon Density of States of High-T_c $Yba_2Cu_3O_7$ with That of the Nonsuperconducting Reference System $Yba_2(Cu_{0.7}Zn_{1.3})O_7$," *Physica C*, Vol. 153–155, 1988, pp. 274, 275.

[15]Ashcroft, N. W., and Mermin, N. D., *Solid State Physics*, Saunders College Publishing, Fort Worth, TX, 1976, pp. 415–450, 466, 467.

[16]Chen, G., "Size and Interface Effects on Thermal Conductivity of Superlattices and Periodic Thin-Film Structures," *Journal of Heat Transfer*, Vol. 119, No. 2, 1997, pp. 220–229.

[17]Phelan, P. E., Song, Y., Nakabeppu, O., Ito, K., Hijikata, K., Ohmori, T., and Torikoshi, K., "Film/Substrate Thermal Boundary Resistance for Er-Ba-Cu-O High-T_c Thin Film," *Journal of Heat Transfer*, Vol. 116, No. 4, 1994, pp. 1038–1041.

[18]Aral, M., Yamada, K., Hosoya, S., Hannon, A. C., Hidaka, Y., Taylor, A. D., and Endoh, Y., "Local Structural Instability of High-Tc Oxide Superconductors Studied by Inelastic Neutron Scattering," *Journal of Superconductivity*, Vol. 7, No. 2, 1994, pp. 415–418.

[19]Roulin, M., Junod, A., and Walker, E., "Scaling Behavior of the Derivatives of the Specific Heat of $YBa_2Cu_3O_{6.93}$ at the Superconducting Transition up to 16 Tesla," *Physica C*, Vol. 260, 1996, pp. 257–272.

[20]Swartz, E. T., "Solid-Solid Thermal Boundary Resistance," Ph.D. Dissertation, Dept. of Physics, Cornell Univ., New York, Aug. 1987.

[21]Chen, G., "Nonlocal and Nonequilibrium Heat Conduction in the Vicinity of Nanoparticles," *Journal of Heat Transfer*, Vol. 118, No. 3, 1996, pp. 539–545.

[22]Folinsbee, J. T., and Anderson, A. C., "The Kapitza Resistance to a Variety of Metallic Surfaces Below 0.3 K," *Journal of Low Temperature Physics*, Vol. 17, Nos. 5/6, 1974, pp. 409–424.

[23]Anderson, A. C., Connolly, J. I., and Wheatley, J. C., "Thermal Boundary Resistance Between Solids and Helium Below 1 K," *Physical Review*, Vol. 135, 1964, pp. A910–A921.

[24]Olson, J. R., and Pohl, R. O., "Kapitza Resistance Between Silicon and Helium-4," *Journal of Low Temperature Physics*, Vol. 94, Nos. 5/6, 1994, pp. 539–550.

[25]Chen, G., "Heat Transport in the Perpendicular Direction of Superlattices and Periodic Thin-Film Structures," *Proceedings of the American Society of Mechanical Engineers-Dynamic Systems and Control Division*, Vol. 59, American Society of Mechanical Engineers, New York, 1996, pp. 13–24.